Effect of Seawater on Carbon Fiber Composite Facings and Sandwich Structures With Polymeric Foam Core

Dayakar Penumadu

1 Introduction

An increasing interest in applying polymeric composites and sandwich layups to ship structures requires a fundamental understanding associated with the degradation of static and fatigue behavior of polymer composites due to long term exposure to marine environment. Stitched cross ply carbon fiber and vinyl ester resin based polymeric composites (facings) and sandwich structures consisting of thick PVC foam core materials with very low density are currently being considered by US Navy and the degradation in mechanical properties of these materials due to harsh naval environment is of high interest.

While extensive data are available for polymers and polymeric composites exposed to sea water environment [1, 2], only a small amount of information has been available for carbon fiber vinyl ester composites and sandwich structures manufactured using conditions relevant to the current needs. It is important to have better understanding that marine composites degrade under sea water exposure. The sorption of water in polymeric composites and their effects on composites' performance is a very complex issue requiring polymer science for fluid interactions with polymer and fiber surfaces at a molecular level and applied mechanics for a detailed understanding of the mechanical response. Issues associated with the mechanical performance of composites and sandwich structures in the presence of water concern their dimensional stability, static strength, fatigue response, performance under blast and impact loading, and delamination aspects of facing-core interface. The utilization of polymeric composite based sandwich structures in naval craft is of current interest to US and several European navies. Typically,

D. Penumadu
Department of Civil and Environmental Engineering, 227 Tickle College of Engineering, University of Tennessee, Knoxville, TN, USA
e-mail: dpenumad@utk.edu

S. W. Lee (ed.), *Advances in Thick Section Composite and Sandwich Structures*,
https://doi.org/10.1007/978-3-030-31065-3_19

those lay-ups are made from load carrying efficient materials consisting of closed-cell polymeric foams placed between fiber reinforced polymeric facings. The resulting sandwich components possess an exceedingly light weight, thereby increasing submersibles' buoyancy and, when employed in superstructure designs, may enhance a ship's stability by lowering its center of gravity. In marine applications, such materials and associated structural components are exposed to sea environment over extended period of time. The degradation in mechanical properties from moisture absorption and temperature variations is a major concern for naval structures.

2 Materials

Three individual materials, closed cell PVC foam, carbon fiber reinforced vinyl/ester facings (composite laminates), and foam-facing sandwich layup structure were considered for the study. PVC closed cell H100 foam material (nominal density of 100 kg/m^3), provided by DIAB, was chosen in this study due to its frequent use in naval sandwich structures [3]. The foam panel was obtained from the vendor in the form of panels with 25 mm thickness. Figure 1 shows an example picture of foam panel, its closed cellular micro-structure, and custom developed tensile/torsional specimens with dumbbell shape for suitable mechanism to grip during a tensile/torsional test, and associated dimensions.

The facing material consisted of stitch-bonded fabric of carbon fiber tows resin infused with vinyl ester. Each carbon tow consisted of 12 k Toray's Torayca T700 individual fibers and the facing was laid up into an equibiaxial fabric. The vinyl ester compatible sizing based fabric, designated by LT650-C10-R2VE, was supplied by the Devold AMT AS, Sweden. The aerial weight of the biaxial fabric was 634 g/sq.m

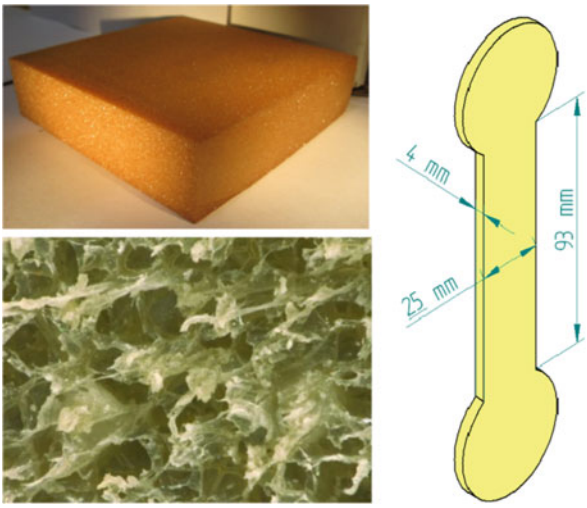

Fig. 1 Polymeric H100 foam

with 315 g/sq.m of fiber in the 0° direction and 305 g/sq.m in the 90° direction. The fibers were stitched together with a 14 g/sq.m polyester knitting thread. Toray's Torayca T700 carbon fiber was chosen because of its cost, stiffness, and strength. From manufacturer's data, the T700 fiber had a tensile strength of 4.9 GPa (711 ksi), a tensile modulus of 230 GPa (33.4 Msi), and an elongation of 2.1%. The matrix material was Dow Chemical's Derakane 510A-40, a brominated vinyl ester, formulated for the VARTM process [4]. The bromination imparts a fire-resistant property to the composite which is essential for ship structures which have a potential to be exposed to onboard fire issue. Vinyl ester has a higher fracture strain than the typical polyesters, and hence produces composites with superior mechanical properties and impact resistance. The fiber volume was found to be 58% by the areal density method and includes 2.2% weight of polyester stitch fiber. Carbon fiber reinforced/vinyl ester laminated composites consisting of $[0/90]_{2s}$ and $[\pm 45]_{2s}$ cross-stitched lay-ups were utilized in this study. Test materials were fabricated following a standard manufacturing protocol using a resin whose viscosity was optimized for Vacuum Assisted Resin Transfer Molding (VARTM) process and all panels were post-cured for consistent quality [4] after infusion and target time of curing at room temperature. The degree of curing was ascertained using differential scanning calorimetry by extracting samples from various locations from a panel.

The sandwich layup consists of a closed cell polymeric foam layer placed between thin carbon fiber reinforced polymeric composite facings that are described above. The composite sandwich panels of size 60 cm × 90 cm (2 ft. × 3 ft) and 2.54 cm (1 in) thickness were fabricated using the VARTM process. Typical test specimens of facing and sandwich beams specimens are shown in Fig. 2.

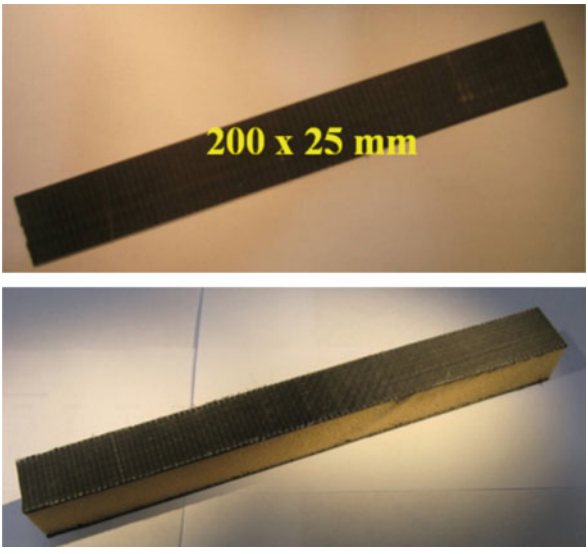

Fig. 2 Carbon fiber reinforced vinyl ester facing (top) and sandwich lay-up made of facing/H100 foam (bottom)

3 Materials Preconditioning to Simulate Marine Environment

To evaluate the effects from sea environment, simulated sea water using coarse sea salt from Frontier with a final density of 1.025 g/cc was used to immerse all samples in controlled water bath at 40 °C. Immersion duration ("Wet" specimens) was decided when they reached a fully saturated state, determined from moisture weight gain data with time. For weight gain measurements, each soaked sample after a given duration was removed from the water bath and patted dry with a paper towel. Micro-scale was used to record the water uptake data prior to determining mechanical properties. Some of the saturated composite coupon specimens were also subjected to low temperature between 0 °C to −15 °C in a freezer or environmental chamber, and subsequently tested at target duration to evaluate cryogenic effect. The test equipment includes an environment chamber that used liquid nitrogen (LN2 and the objective was to understand the material behavior as function of aging condition at cryogenic temperature in sea water environment to mimic the exposure of ship structures in extreme cold temperatures.

4 Seawater and Temperature Effects on Constituent Materials

Polymeric H100 foam

A biaxial servo-hydraulic mechanical testing MTS 858 system with a full-scale capacity of 25 kN axial force and 250 N-m torque was fitted with an external 110 N (25 lbf) axial load cell for tensile tests and a 0.7 N-m torque load cell for torsional tests to conduct mechanical tests on PVC foam core material. To obtain tensile modulus of foam core, extension tests were performed at strain rate of a 0.5 mm/min and up to a peak stress of 0.6 MPa, a state of stress that is well below the non-linear stress-strain relationship. In a view of previous experience, each specimen was subjected to three load/unload cycles at room temperature to establish a repeatable value of Young's modulus, E. Subsequently, the same specimens was immersed in sea water roughly 2 months and frozen down to a temperature of about −5 °C in a freezer and tested in tension after exposure duration of 2 and 6 weeks, respectively. It is important to test the environmental effects on the same specimen due to large variation in properties of foam coupon specimens obtained from same panel. The properties also vary through thickness as will be noted below.

Based on previous research, it was concluded the sea water penetrated only the outer cellular layer of the foam. This explains why tensile mechanical properties were insensitive to the presence of sea water as discussed in the next section. Therefore, a torsion test, used to measure shear modulus G, was deemed to be more likely to capture the effects of sea water, since in that test the highest shear stresses develop at

the outer locations of the prismatic shaped specimen. Ten specimens were used to determine freezing effects on dry specimens and additional 10 specimens were prepared and used to test wet specimens which were soaked in sea water for 8 weeks and tested at room temperature. These wet coupons were subsequently kept in a freezer at −5 °C for 4 weeks and tested again in torsion. A rotation range of $-5^\circ \leq \theta \leq 5^\circ$ at rate of 10 degree/min was used to study the effects of sea water and low temperature on the shear modulus G of foam. These values of rotation correspond to shear strain values well below yield state of stress.

Carbon vinyl/ester facing laminates

Tensile tests were performed on 200 mm long and 25 mm wide specimens and approximately 2 mm thick to determine the effect of freeze/thaw cycling on the Young's modulus, E of $[0/90]_{2s}$ and $[\pm 45]_{2s}$ layups. An MTS 810 test system with 250 kN load cell was employed under strain control at rate of 300 με/min and up to 750 με, which is well within the linear elastic axial strain level. Failure strength test was also performed using the same equipment and procedure. Strains were recorded by an extensometer. Tabs were mounted at the ends of the specimens, in order to direct failure away from the stress concentrations at the gripped portions. Prior to the tensile tests, all the specimens were completely dried at ambient temperature in desiccators.

The facing specimens were enclosed within an environmental chamber connected to liquid nitrogen to evaluate the low temperature effect on water soaked specimens. Note that, as desired, the profile was controlled to vary between the ambient temperature down to 0 °C, −15 °C, and then back up to 0 °C, with a final return to room temperature. Each of the above temperature levels were maintained for at least 2 h. The sample was held at zero load in the servo-hydraulic system throughout the thermal excursions to allow for free thermal expansion (or shrinkage).

Foam/facing interface fracture toughness

The composite sandwich panels of size 60 × 90 cm as mentioned above were cut and machined to form 254 mm long, 25.4 mm wide, and approximately 29 mm thick sandwich specimens. In addition to the foam and facings, the thickness dimension included also the thickness of top and bottom adhesive interfaces. Fifty millimeter long pre-cracks were cut with a sharp edge along the top facing/core interface in order to stimulate the growth of the interfacial delamination [5]. Load application was facilitated by using hinges glued to the facings in a modified double cantilever beam (DCB) configuration which was followed the procedure in previous work [6]. The hinges were mounted 38 mm away from the edge of the loaded, top, facing and the sandwich specimens were centered about the sides of the steel plates. The effect of exposure to sea water on fracture toughness was investigated by pre-soaking the specimens for 3 months in simulated sea water using natural coarse sea salt at a controlled temperature of 40 °C in a water bath prior to the initial delamination testing. Subsequently the specimens were soaked for interim periods of 2 weeks during intermittent crack growth between unloading and reloading cycles. It was necessary to re-soak each "wet" specimen for at least 2–3 weeks, in order to

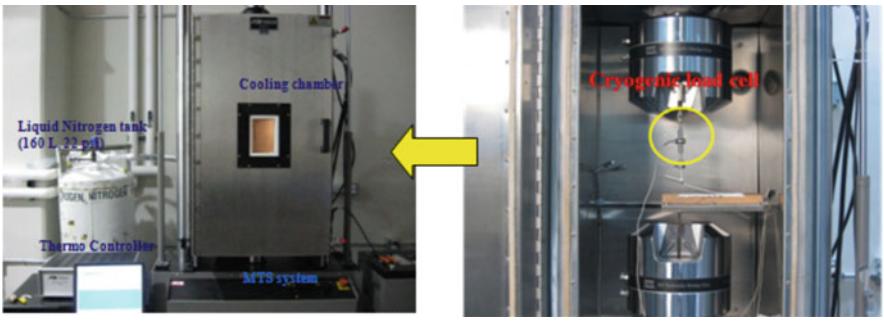

Fig. 3 Delamination test set up including an environmental controlled chamber

maintain a fully saturated crack tip region after each unloading and prior to each reloading.

A 250 kN MTS test system was employed in combination with an MTS 609 alignment fixture and a smaller 50 kN axial force transducer. Loading was introduced by means of the larger, 250 kN, MTS machine under displacement control at a crosshead rate of 2 mm/min. The specimens were placed an inside environmental chamber, within which was encased custom made fixture attached to 1 kN cryogenic tensile load cell perform delamination tests as shown in Fig. 3. Programmed loads were monotonically increased under displacement control until noting an abrupt drop in their amplitudes, at which stage crack extensions were observed and the machine unloaded back to zero displacement. This procedure was repeated until delamination's approached the far edge of a specimen. The digital images of the interfacial cracks were analyzed using digital image analysis software (ImagePro®). Crack morphology was also determined for possible use in calculating values of critical energy release rate. This was done by transferring the gray scale image to binary form using thresholding technique and by focusing on the region of crack-tip. The exact length of crack was obtained by tracking the number of pixels and conversion to length units using the known optical magnification at which digital images were obtained.

Tensile modulus of foam

Figure 4 depicts the typical loading data of PVC foam and a custom made fixture and setup. Based on previous experience, each specimen was subjected to three load/unload cycles to establish a repeatable value of E. The modulus was obtained from averaging only the second and third load cycles, since those presented almost identical information. Table 1 shows average tensile modulus value from 20 specimens at up to the same target stress level. The data for the same tests, conducted after 2 and then 6 weeks exposure to -5 °C, exhibit no degradation in the values of E. It can be seen that exposure to low temperature over period of time does not significantly affect the value of E for specimens. The minute degradation of E falls well within the data scatter caused by foam inhomogeneity. Foam specimens were tested before immersing in seawater for 10 weeks and tested at room temperature to obtain

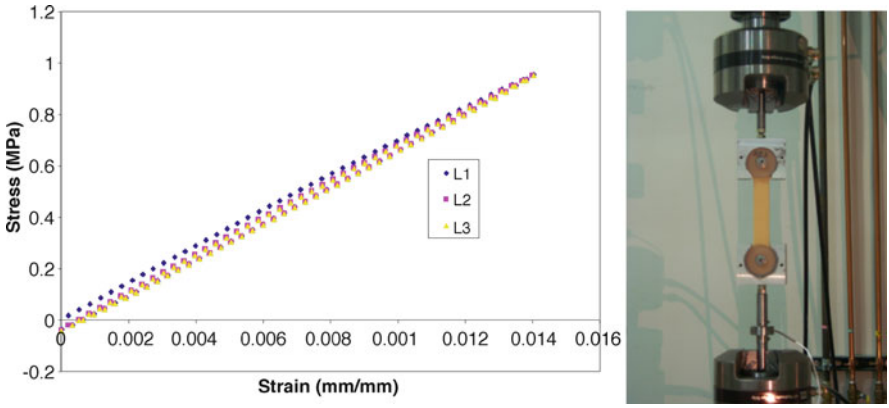

Fig. 4 Typical three cycles used to determine *E* modulus and tensile test set up

Table 1 Low temperature effect on foam modulus in tension

Condition	Room	0 °C (2 weeks)	0 °C (6 weeks)
Dry	70.66 MPa	70.84 MPa	70.42 MPa

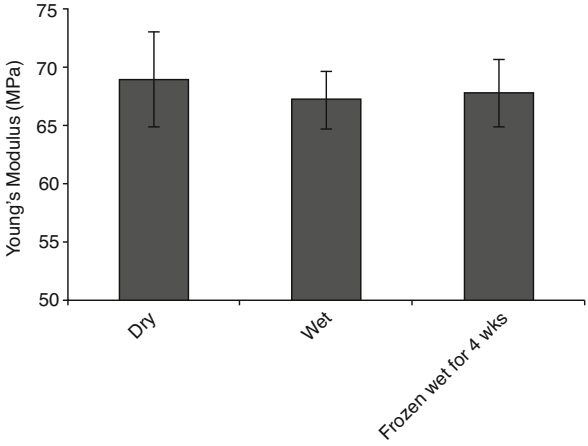

Fig. 5 Summary of tensile modulus variation of H100 PVC foam before/after sea water saturation and freezing for 4 weeks

comparative values of *E*. It was noted the sea water causes approximately 5% degradation in *E*. Subsequently, those "wet" specimens were frozen for 4 weeks and tested in tension to obtain the corresponding values of *E*. The data yielded nearly identical results before and after freezing as shown in Fig. 5.

For carbon fiber vinyl/ester facing, tensile tests were performed on 200 mm long and 25 mm wide specimens to determine the effect of freeze/thaw cycling on the Young's modulus, *E* of $[0/90]_{2s}$ and $[\pm 45]_{2s}$ layups. The tensile modulus was determined from the slope of the stress-strain curve in elastic range prior to yield. In the dry state, the facing composites were found to have approximate average

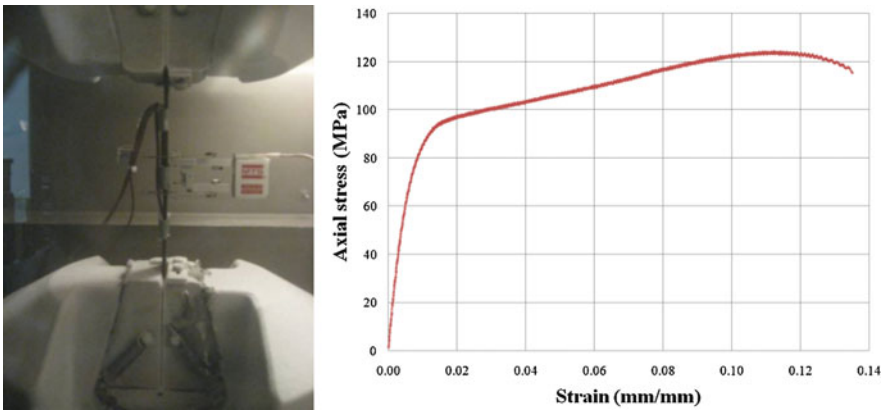

Fig. 6 Low temperature setup and behavior of $[\pm 45]_{2s}$ carbon fiber vinyl ester facing

moduli of elasticity of 80 GPa and 15 GPa, respectively. Figure 6 shows the setup of a tensile test and a typical stress-strain result. In a view of authors' past research to evaluate environmental effects, $[\pm 45]_{2s}$ facing layup show more pronounced degradation; therefore, this study focused only on this specific orientation of facing, where resin behavior also comes into play and thus most vulnerable for environmental effects. The initial values of E were ascertained by subjecting each specimen to three cyclic tests prior to thermal exposure, resulting in 15 GPa $\leq E \leq$ 16.5 GPa.

A similar procedure was employed to record values of E after the aforementioned exposure to cyclic temperature. The sea water effect was evaluated by pre-immersing the sample at 40 °C at least 3 months and recording E immediately upon their removal from the bath. It was noted that immersion caused only small differences in properties of the $[\pm 45]_{2s}$ facings. A similar procedure was employed to record values of E after exposure to sea water and cyclic low temperature. After measuring stiffness immediately upon their removal from the bath, it was followed by freezing the wet specimens at −10 °C for 2 weeks and obtaining the subsequent values of E inside chamber.

The procedure was repeated 6 weeks later. To simulate a cold environment, the target temperature in the chamber was held roughly 2 h before testing. The overall results were close to those of dry facing where the average stiffness at low temperature increased by 3–5% at −10 °C beyond those of the dry specimens as shown in Fig. 7. The slightly increased values are possibly attributed to an improved mechanical factor by the generation of thermally induced internal compressive stresses within the $[\pm 45]_{2s}$ coupons which enhance the friction between the contracting resin and the fibers.

Shear modulus of foam core material

The shear modulus G was recorded by means of torsional tests, twisting the sample over the angular range of $-5^\circ \leq \theta \leq 5^\circ$. The base-line variability ranged between 23.3 MPa $\leq G \leq$ 28.9 MPa tested under torsion at room temperature. It was

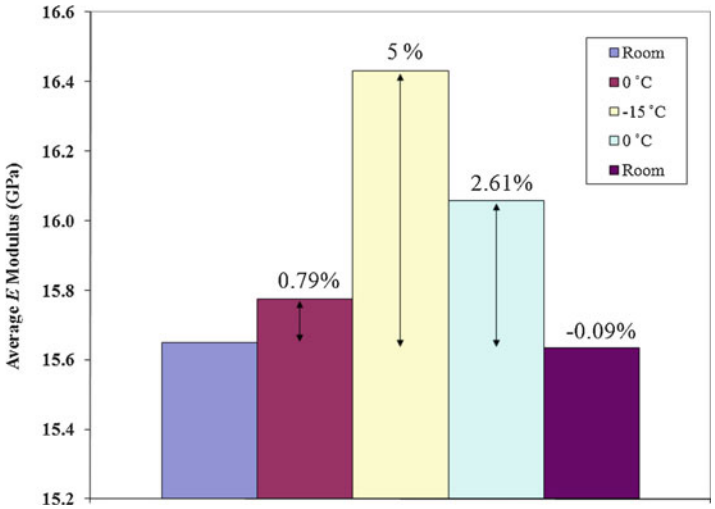

Fig. 7 Average values of dry elastic modulus for composite facings (45 degree orientation) subjected to low temperatures

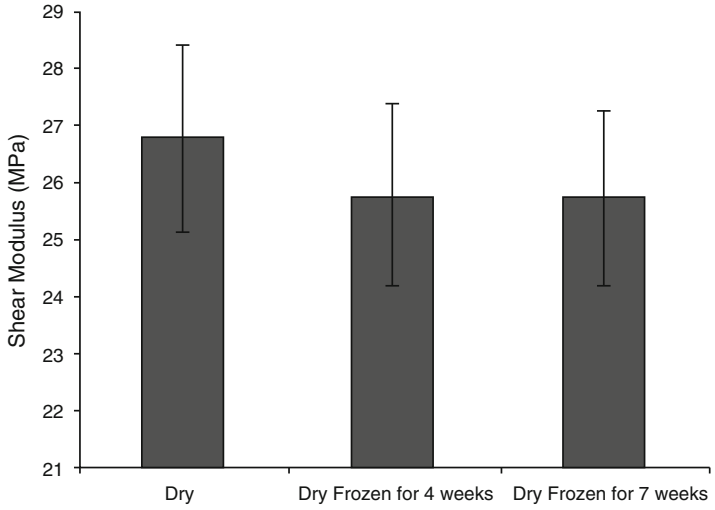

Fig. 8 Shear modulus before/after freezing

necessary to establish their reference values for a comparative purpose. Shear modulus values for 10 specimens tested in the dry state exhibit fairly comparative reductions from room temperature levels down to those due to subsequent freezing for 4 and 7 weeks. Reductions of shear modulus 3–6**%** were noted after 4 weeks of freezing and no further drop at 7 weeks shown in Fig. 8.

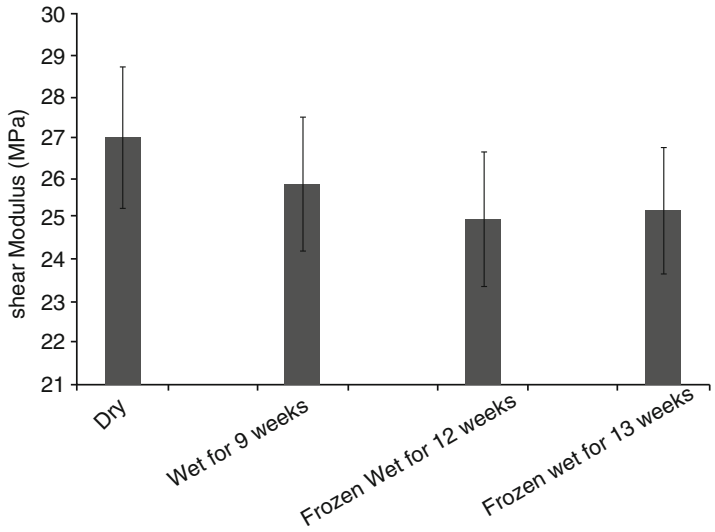

Fig. 9 Shear modulus due to sea water and low temperature

Additional ten specimens were used to study the combined effects of sea water and cryogenic temperature. The results in Fig. 9, show an overall degradation of 5% with a further of slight decrease around 2% after freezing for additional 13 weeks. Immersion in sea water resulted in an overall reduction of up to 5% in G, though it should be borne in mind that this reduction is affected by sea water that is confined to a region that is only 0.4–0.5 mm (δ_T) deep along the outer boundary of the specimen.

To evaluate the wet shear modulus of the foam G_w [7], Fig. 10 shows all known dimensions and materials properties, except G_w. Employing the well-known expression relating the torsional behavior of a solid rectangular sections of height D and width W, and a similar relationship for a hollow rectangular tube of the same outer dimension and thickness δ_T. These are

$$\left[\frac{M_T^{(s)}}{\theta}\right]_{solid} = \frac{1}{3} H_s h_s^3 G_s \text{ and } \left[\frac{M_T^{(o)}}{\theta}\right]_{hollow} = \frac{4A^2 G \delta_T}{L} \tag{1}$$

where $A = (D - \delta_T)(W - \delta_T)$ and $L = 2(D + W - 2\delta_T)$

The saturated sample consist of an inner, essentially dry, core of modulus G and dimensions $H_s = D - 2\delta_T$ and $h_s = W - 2\delta_T$. This core is encased within a thin saturated tube of thickness δ_T. Denote by R the ratio $\left(\frac{M_T}{\theta}\right)_{dry} \Big/ \left(\frac{M_T}{\theta}\right)_{wet}$. One obtains

$$R = \left(\frac{H_s}{D}\right)\left(\frac{h_s}{W}\right)^3 + \frac{12A^2\delta_T}{LDW^3}\frac{G_w}{G} \tag{2}$$

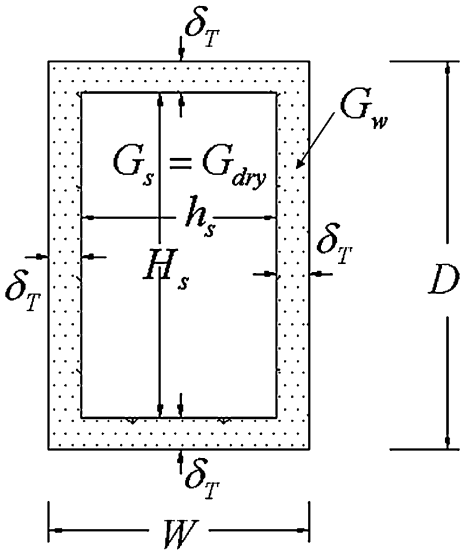

Fig. 10 A sketch of the cross section subjected to torsion. Note that G_{dry} and the overall torsional resistance are experimentally determined. The only unknown is G_w of the saturated region

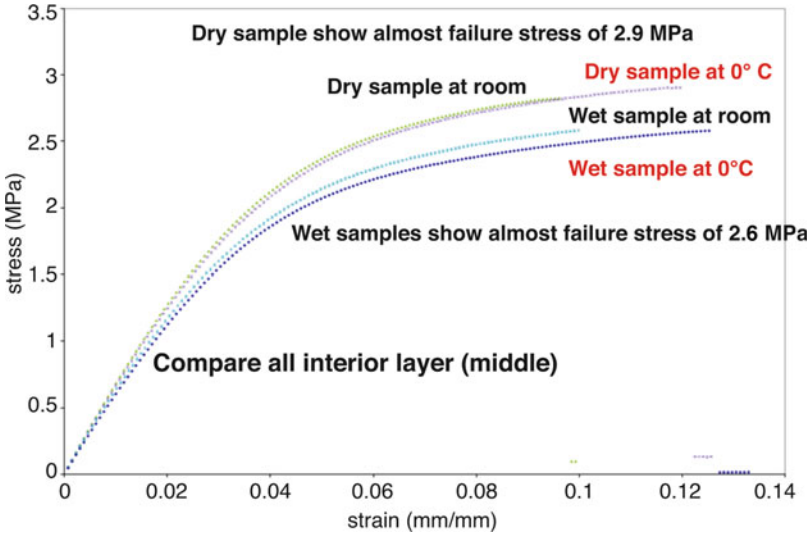

Fig. 11 Comparison of failure stress of PVC foam subjected to sea water effect

In summary, it was shown that low temperature and sea water do not significantly reduce tensile properties but that the overall shear modulus had decreased by 7% at sub-zero temperature.

Failure strength of foam core material and matrix dominated facing

Strength of PVC foam under tensile test indicated an average value of 2.5 MPa in virgin state of the materil. Figure 11 shows a general trend of polymeric foam

Table 2 Critical energy release rate for interface delamination of face sheet and PVC foam core

Condition (No of samples)	G_c (Front) (N/m^2)	G_c (Back) (N/m^2)	% Avg. Degradation
Dry (> 15)	580–952	541–963	
Wet (> 10)	432–619	451–632	~30%
Cyclic wet frozen (>8)	405–690	420–620	No additional degradation

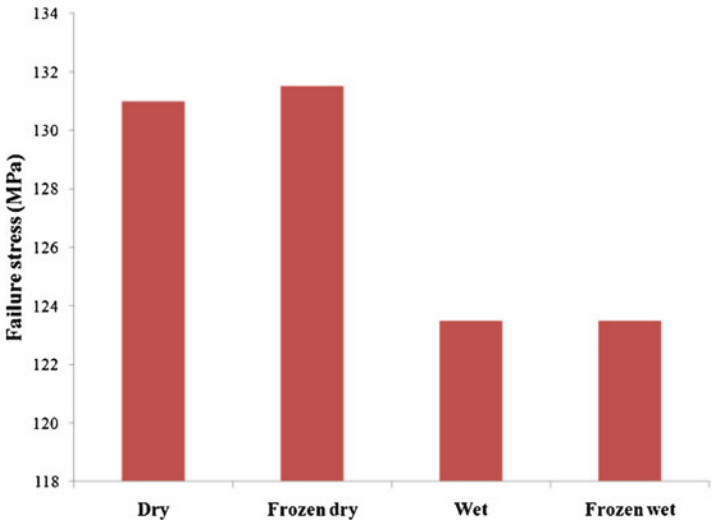

Fig. 12 The $[\pm 45]_{2s}$ degradation of failure stress before/after exposed to sea environment and low temperature

subjected to sea water and low temperature. The results in Table 2 show that the sea environment could degrade the strength up to 10% and combined effect of sea water and low temperature only slightly degrades further.

Comparative study on carbon fiber reinforced vinyl/ester facing shows that strength data of facing for coupons extracted along $[\pm 45]_{2s}$ yielded approximately 130 MPa and no difference resulted in exposure to low temperature, but a further decrease of 5% due to sea water effect. No further significant reduction shows on combined effects of sea water and low temperature. Comparative results are summarized in Fig. 12.

Delamination of face-foam core for sandwich material

The resistance to delamination growth can be characterized by the strain energy release rates (G), where the critical energy release rate (G_c) is used as a measure of the interminar fracture toughness. Assuming a linear elastic response, it was chosen to determine the critical strain energy release rates G_c by means of the "area method". The area under each load/unload cycle was calculated numerically using

the trapezoidal rule. Critical energy release rate, which defines the fracture toughness, was obtained using the expression:

$$G_c = \frac{1}{b} \cdot \frac{\Delta U}{\Delta a} \tag{3}$$

Where ΔU is the area under the load-displacement trace as the crack grows; Δa is the extended crack length recorded during the test, and b is the width of specimen. The value calculated is the average energy consumed for the crack extension Δa. The wide range of values listed in Table 2, where values are listed for crack lengths observed on both sides of the specimens, reflects the cycle to cycle variability in the thickness of the facings as well as the random nature of the foam cell structure. Accordingly, exposure to sea water resulted in approximate 30% reduction in G_c and exposure to combination of sea water and cryogenic temperature slightly degrades it. These results indicate that exposure to sea environment significantly reduces the interfacial toughness between facings and foam core material.

5 Effect of Seawater and Microstructure on Composite Laminates (Facings)

CF/VE specimens were prepared using different ply lay-ups, namely $[0/90]_{2S}$ and $[\pm 45]_{2S}$ as described earlier to achieve fiber and matrix dominated failure respectively. Tensile tests were performed under deformation control at a constant crosshead rate of 0.1 mm/min, at room temperature in air. In order to minimize the effect of gripping stress on the mechanical behavior and to avoid failures within tab section, 25 mm long tabs were attached to the ends of the specimens using a suitable adhesive. Where experimentally feasible, an extensometer was used to record strain data for comparison purposes. It showed comparable results with Digital Image Correlation (DIC) technique used to obtain surface strain data.

The DIC system (commercially available, VIC-3D) uses dual-cameras to measure surface displacements, and full-field surface strains in three dimensions (Fig. 13). Mechanical properties of carbon fiber reinforced vinyl ester composites (CF/VE), consisting of fiber dominated samples of $[0/90]_{2S}$ and matrix dominated samples of $[\pm 45]_{2S}$ orientation, using variable specimen sizes were evaluated.

Fiber and matrix dominated specimens, $[0/90]_{2S}$ and $[\pm 45]_{2S}$ repectively, showed similar stress-strain behavior for all sample sizes considered in this study. No damage was found until catastrophic failure as shown in Fig. 14(a) for fiber dominated specimens corresponding to $[0/90]_{2S}$ lay-up. The strain information reported in these stress-strain curves was obtained using DIC technique. Figure 14(b) shows the deformation behavior for a matrix dominated specimen, showing significant damage accumulation beyond 80 MPa axial stress. Typical mechanical properties of fiber and matrix dominated carbon fiber reinforced vinyl ester composites can be found in Table 3.

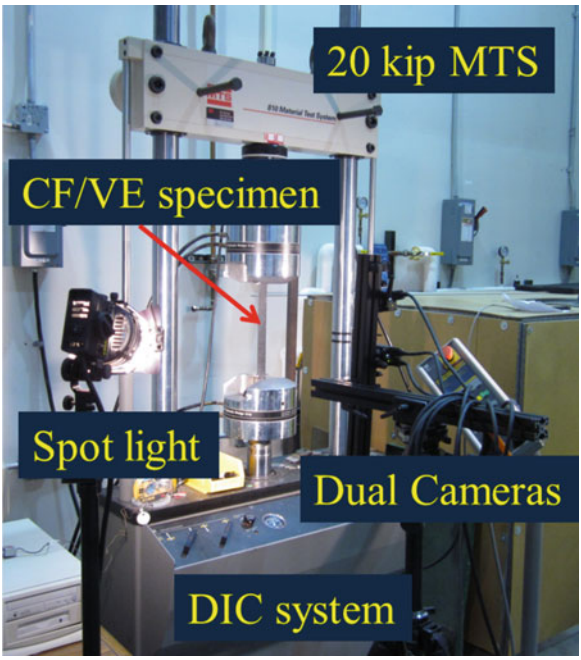

Fig. 13 Experimental set-up for a tensile test using a servo-hydraulic loading system, coupled with DIC system for obtaining strain data on the specimen surface

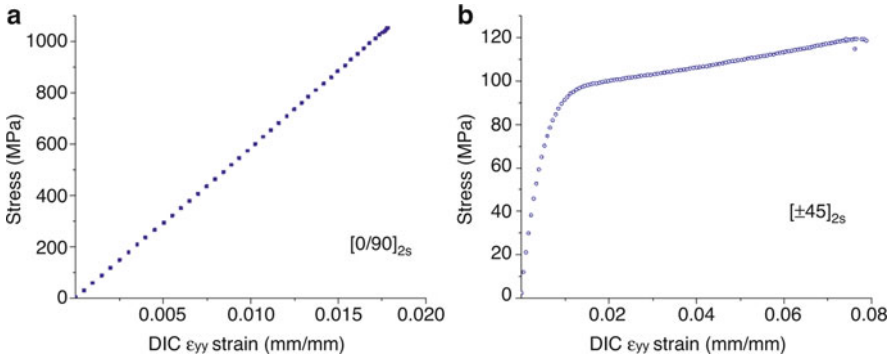

Fig. 14 Typical stress-strain behavior of (**a**) fiber $[0/90]_{2S}$ and (**b**) matrix $[\pm 45]_{2S}$ dominated CF/VE sample dimensioned 300 mm long by 25 mm wide

Table 3 Typical material properties of CF/VE composite facings

Property	Value	Dimension
Longitudinal modulus $[0/90]_{2S}$	60	GPa
Longitudinal modulus $[\pm 45]_{2S}$	15	GPa
Failure strength $[0/90]_{2S}$	1000	MPa
Failure strength $[\pm 45]_{2S}$	120	MPa

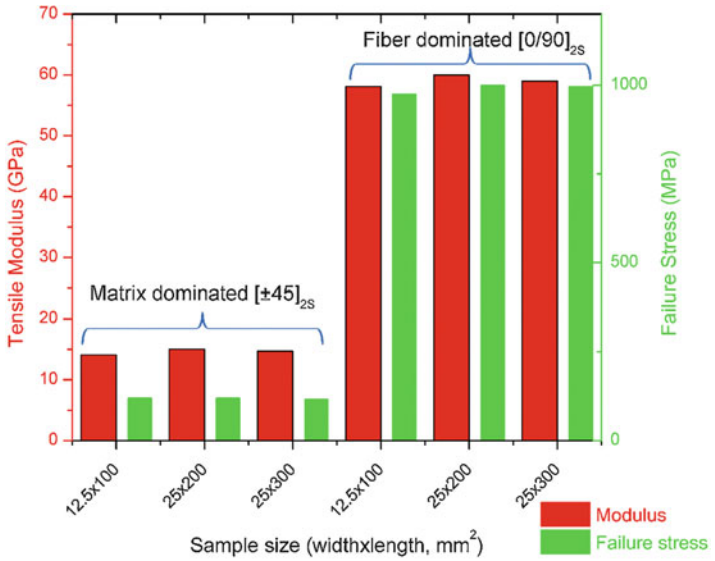

Fig. 15 Effect of specimen size on mechanical properties of laminates

CF/VE specimen sizes were scaled up of 2 and 3 from the baseline case with keeping the constant thickness from same four cross stitched plies (2.8 mm). The large size of both fiber and matrix dominated specimen showed similar strength and moduli as summarized in Fig. 15.

Using the observations obtained from strain variations using 3D-DIC, it is concluded that the failure of the CF/VE samples are dominated by strain localization (Figs. 16 and 17) possibly from manufacturing defects sites expected of VARTM technique and specimen size effects were not significant. Since strength and moduli are controlled by defects, especially voids and manufacturing defects associated with varied amount of cross-link density and fiber interfacial shear strength during specimen preparation, it is crucial to make sure that good manufacturing quality of test specimens is achieved in production. A fundamental question of why certain zones lead to large accumulation of strain localization for the carbon fiber composites was further explored by a using x-ray based tomography in non-invasive mode.

CF/VE samples were also subjected to controlled rate of strain loading with ten tensile load-unload loops (corresponding to unloading at 20, 40, 60, 80 MPa, and 5 loops at 100 MPa) to evaluate accumulated plastic strain as shown in Fig. 18a. Fiber dominated CF/VE $[0/90]_{2S}$ composites under ten cycles of up to 80% failure stress load-unload did not show accumulated permanent strain.

In order to evaluate the damage evolution due to sea water effects compared to time aged sample, a saturated CF/VE $[\pm 45]_{2S}$ that was soaking in sea water for 3 years was also subjected to similar testing. This particular sample had a moisture uptake of 0.8% based on periodic weight gain measurement. Results included in Fig. 18 shows that exposure to sea water substantially increased the damage measured at various strain or stress levels quantifying the relative effect of marine

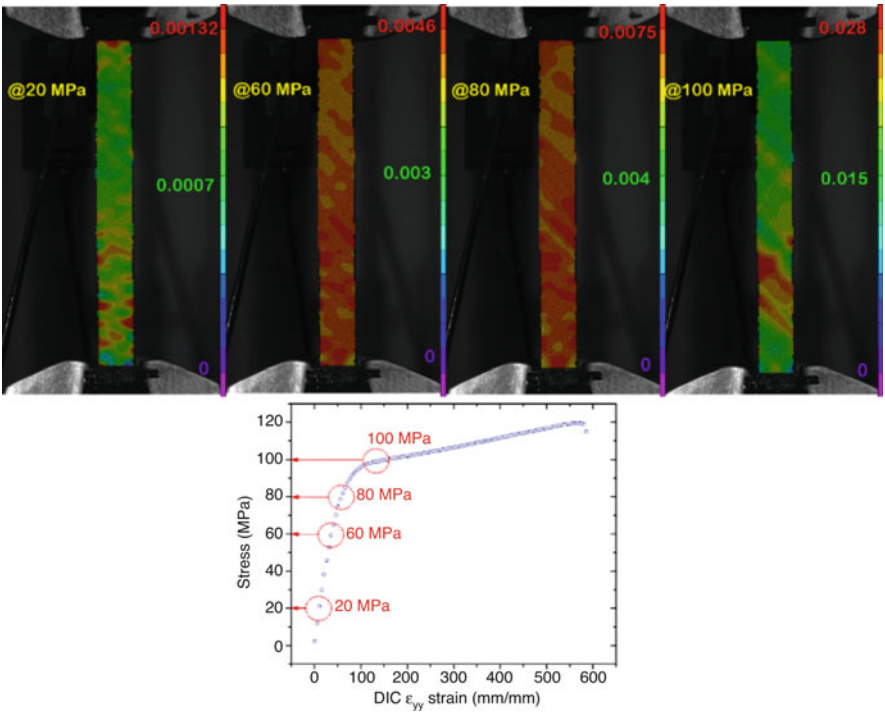

Fig. 16 Deformation variation of matrix dominated CF/VE using major principal strains at various specific stress levels

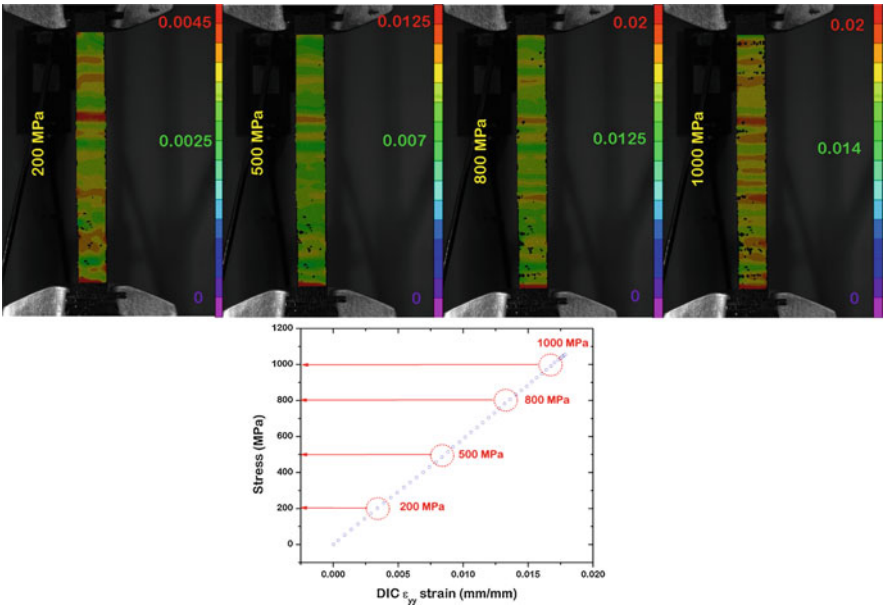

Fig. 17 Deformation variation of fiber dominated CF/VE using major principal strains at various specific stress levels

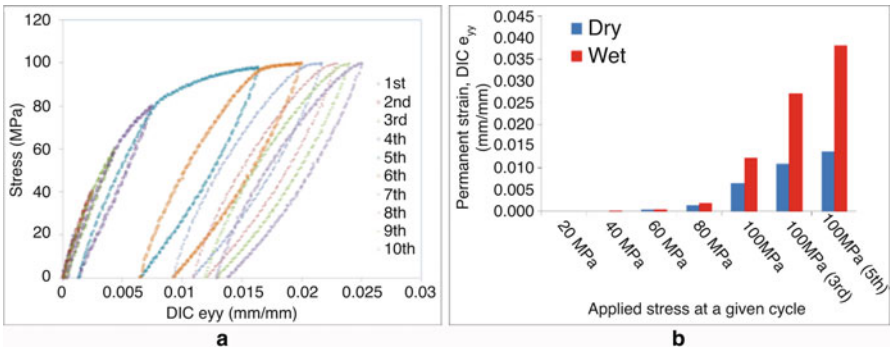

Fig. 18 (**a**) Typical load-unload behavior of undamaged $[\pm 45]_{2S}$ CF/VE, **(b)** Damage evolution of "wet" and dry matrix dominate CF/VE subjected to tensile load-unload varying from first cycle to 10th cycle

environment on damage evolution. After 10 cycles of tensile load-unload, saturated $[\pm 45]_{2S}$ CF/VE sample showed substantial matrix cracking on the sample surface unlike the case of dry and aged specimen of $[\pm 45]_{2S}$ CF/VE composite. Corresponding to the 10th load-unload cycle at the amplitude of axial stress prior to unloading of 100 MPa, large strain variations along the sample length with high strain localization at mid height were observed.

6 Fatigue Behavior of Sandwich Facing Material and Seawater Effect

Under tension-tension fatigue test, orientation dependence of CF/VE exhibit disparate failure mechanisms when fatigued in air or under immersed conditions that lead to earlier failures when submerged in fluid. The secant and tangent modulus, E_S and E_T respectively were used to determine the degradation due to sea water confinement effect at each orientation [8–12]. The fatigue life of composites is denoted by the number of load cycles to failure defined as a target state of strain accumulation or catastrophic failure. It was observed when comparing peak strain subjected to same stress level of $0.5 \times \sigma_{failure}$ between fiber and resin dominated composite laminates, sea water confined effects did not significantly reduce fatigue life on fiber dominated specimens. On the other hand, sea water confinement has a significant effect to reduce fatigue life on resin dominated CF/VE. In the present research, tangent moduli comparison between fiber and matrix dominated CF/VE at the same stress level of $2/3\sigma_{failure}$ showed the similar observation as mentioned above. Note that a cyclic fatigue tests were suspended when 1 millions of cycles were achieved. This fatigue endurance limit was used in several studies in the past [12, 13]. Based on the results, only matrix dominated samples are considered for detailed studies on degradation in fatigue life due to seawater exposure and confinement.

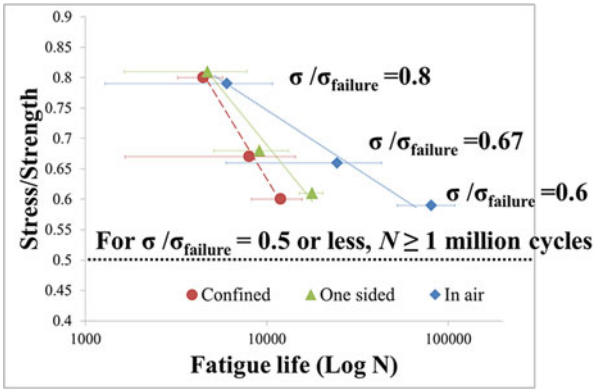

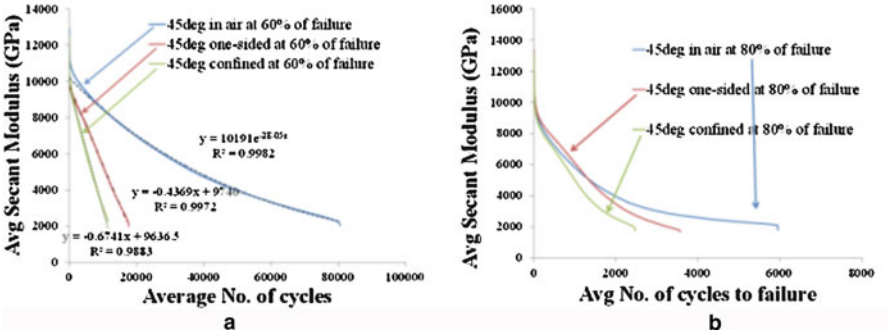

Fig. 19 Fatigue life of $[\pm 45]_{2S}$ CF/VE in air, and water confinement

Fig. 20 (**a**) Fatigue life data of $[\pm 45]_{2S}$ CF/VE to in air, water confinement, and one-sided confined, (**b**) Secant modulus degradation model using simple regression analysis

Fatigue life of CF/VE composite samples on $[\pm 45]_{2S}$, which have the average static failure strength at 120 MPa, were obtained at maximum applied stress levels of 0.8, 0.67, 0.6, and 0.5. Fatigue life due to sea water confinement and one-sided confined effects are summarized in Fig. 19 when compared to cyclic loading in air. A significant degradation of number of cycles to failure from sea water confinement effects was observed for all stress levels considered in this study, up to 80% of static strength as the maximum cyclic stress value for a stress ratio value R of 0.1. Prediction of fatigue life in composites is very complicated because of multiple failure mechanisms possible including fiber interface initiated damage, fiber breakage, matrix cracking and associated debonding. With different damage accumulation mechanisms in composites, secant modulus degradation as in Fig. 20a from measured data was found to be a representative and simple parameter to provide tension-tension fatigue life prediction. Due to water confinement effects a simple linear regression based predictions will provide an adequate estimate of number of cyclic failures and the fatigue life available. However, accumulated fatigue damage of CF/VE using secant modulus degradation in air does not appear to show this linear dependency with cycles of loading. These results are important to develop the

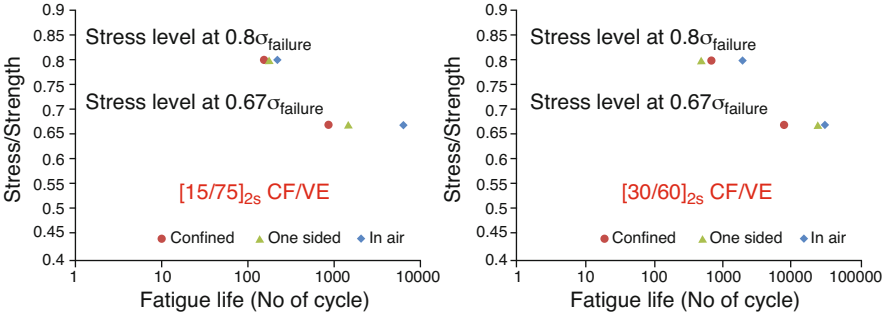

Fig. 21 Fatigue life data of $[15/75]_{2S}$ and $[30/60]_{2S}$ CF/VE due to in air, water confinement, and one-sided confined

endurance fatigue limit for use in marine design. Similar observations were found in $[15/75]_{2S}$ and $[30/60]_{2S}$ from Fig. 20b and the number of cycles to failure reduced considerably when compared to dry condition in air. True strain data prior to failure showed a similar trend when comparing dry sea water confinement or one-sided confined samples to dry in air samples.

Comparison of experimental results for $[15/75]_{2S}$, $[30/60]_{2S}$, and $[\pm 45]_{2S}$ laminates of CF/VE composites yielded failures under much fewer numbers of cycles at $2/3\sigma_{failure}$ when fatigued under completely immersed conditions than in air can be found in a previous year report. Fatigue life of $[15/75]_{2S}$ and $[30/60]_{2S}$ due to sea water confinement is compared in Fig. 21. It was supported by X-ray tomography results that the damage development in matrix dominated samples is the combination of the coalesced matrix cracks parallel to the fiber and delaminations; however, voids between matrix/fiber rapidly grow and lead to the early fatigue failure mode when confined in sea water. Fatigue behaviors of CF/VE at various orientations as function of stress levels and different R-ratio have been considered and master curves developed for naval design applications.

7 CFVE Sandwich Structure Fatigue Behavior Exposed to Sea Water

Past research on CFVE sandwich structure response has been focused largely on delamination fracture testing and response from three/four point bending. Those studies involved fiber dominated CFVE sandwich materials in the experiments. It is important to consider matrix dominated sandwich structures, especially under water confinement conditions due to the large role matrix resin plays in damage evolution under fatigue loading in tension. Recent work of the author showed that water confinement effects are very pronounced for matrix dominated CFVE results. Therefore, similar experiments were conducted, now using actual sandwich structures in matrix dominated mode, and results are being evaluated by comparing

Fig. 22 Experimental set-up with dry matrix dominated CFVE sandwich specimen

fatigue response of dry vs. one sided immersion in terms of cyclic fatigue life (No of cycles) and associated damage evolution.

The experimental setup shown in Fig. 22: Experimental Set-up with Dry Matrix Dominated CFVE Sandwich Specimen setup was utilized for this research to evaluate tensile fatigue behavior using specimens with a total length L of 225 mm, a gage length GL of 150 mm, and a width w of 25 mm. A 3-D DIC system described earlier was used to obtain spatially resolved strain as a function of the state of loading. Figure 23 shows the setup for one-sided exposure to seawater using a latex bag to make water available while the composite facing is undergoing cyclic loading. Due to water available during loading, as matrix cracks develop, water wicks into these cracks and causes crack coalescence and growth quickly, thus causing large loss in fatigue life with one side of the sandwich panel exposed to seawater, a condition very similar to actual ship structure in the ocean.

Four or more samples in each case were evaluated to infer the sea water confinement effects. Figure 24 shows a typical tensile result of 2 ply CFVE sandwich structure studied in unison with spatially resolved tensile strain during monotonic loading. A relative comparison of modulus and failure strength in tension of 2-ply sandwich CFVE composites and typical 4-ply CFVE laminate are summarized in Table 4. The large decrease in modulus and failure strength is partially due to reduction in fiber volume fraction and changes in degree of cross-linking and matrix properties due to change in cure kinetics with PVC foam having some influence on the cross-linked state of vinyl ester resin (Fig. 25).

Tensile fatigue life of 2-ply CFVE sandwich composites while sea water was allowed to interact with composite sandwich specimen on one of its outer faces was found to substantial decrease (56% due to sea water confinement) as shown in Fig. 26. Fatigue life of CFVE sandwich composites with matrix dominated samples due to sea water confinement effects were obtained in this case at a stress level of 0.67 based on previous study of the author in evaluating laminate behavior by in isolation.

Fig. 23 Matrix dominated wet CFVE specimen with one-sided water confinement

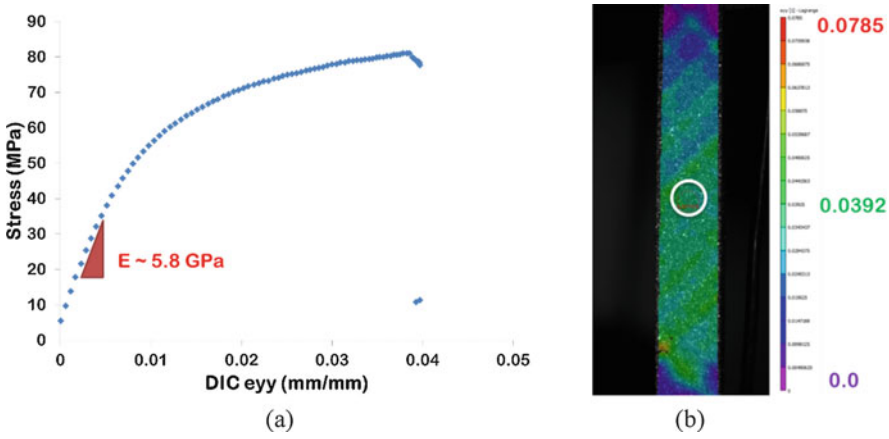

Fig. 24 CFVE sandwich structure subjected to tensile loading coupling DIC results

Table 4 Typical results of 4-ply and 2-ply matrix dominated $[\pm 45]_{2S}$ CFVE

Conditions	Average modulus (GPa)	Failure stress (MPa)
4-ply dry CFVE $[\pm 45]_{2S}$	15	120
2-ply dry CFVE $[\pm 45]_{2S}$	5.8	84.5

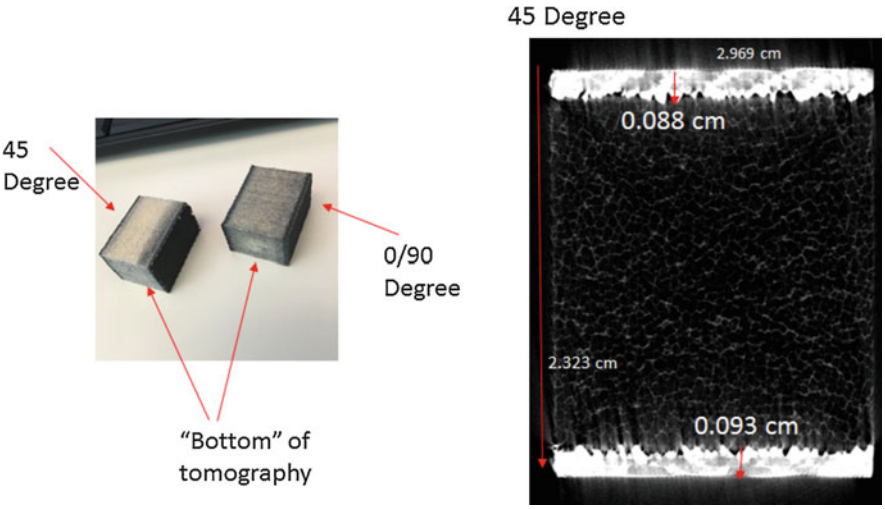

Fig. 25 X-ray computed tomography of sandwich facing and foam core showing resin rich areas with lower fiber volume fraction and saw-tooth microstructure resulting in large stress concentrations during cyclic loading

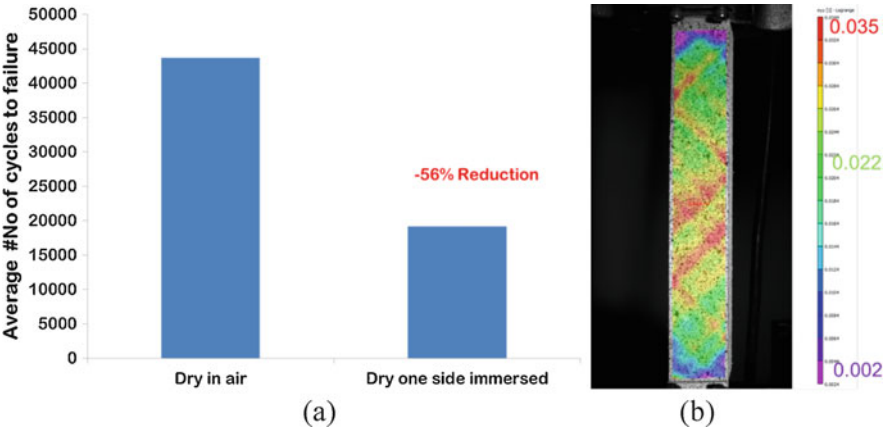

Fig. 26 (**a**) Comparison of matrix dominated CFVE dry in air and dry with one sided water confinement, (**b**) Typical DIC strain results along the sample length

8 Compressive Behavior and Seawater Effects

The complex behavior of CFVE composites subjected to tensile loading in monotonic and cyclic conditions and seawater effects have been addressed in the previous sections of this chapter. The associated degradation from the isolated and coupled effects of sea water, hydrostatic pressure, and cold temperature were also summarized. Since naval designs incorporate vinyl ester resin due to its superior performance in sea environment compared to epoxy based system, due to its low cost, and tunable properties for interface with a given sizing of considered carbon fiber type and intermediate form as stich bonded fabric, and VARTM manufacturing technique is well suited for naval needs, it is important to understand and evaluate this material system for particular manufacturing conditions in compression also. Such data and three dimensional behavior does not exist in the literature. It is also not clear how the sea water diffused CFVE system will degrade under compression. It is to be expected that the mechanical response of the CFVE will be very different in compression compared to tension and matrix will have a larger effect than in tensile loading, with corresponding degradation effects from marine environment potentially more significant. Compression behavior of fiber reinforced composites has proven to be a very important but poorly understood aspect fiber reinforced composites and over the years there has been a considerable lack of understanding on best ways to measure it experimentally. This led to the development of Combined Load Compression (CLC) approach as the test fixture is easier to use, repeatable to manufacture, and less massive than the Illinois Institute of Technology Research Institute (IITRI) developed compression fixture.

Standards exist for both approaches (ASTM D 6641 and D 3410). CLC test fixture (Fig. 27) is more recently widely adopted by the composites industry as the fixture is small, relatively easy to fabricate, and the combined use of end loading and shear loading in the grip region leads to more uniform state of compressive stress in the gage section. A key advantage is also that the use of tabs are avoided for the specimen, thus if a high degree of care was taken in ensuring uniform thickness samples during fabrication, eccentricity in the load train and resulting in bending stresses is minimized further. A specimen with a gage length of 12.7 mm and an overall size of 5.5″ (140 mm) × 0.5″ (12.7 mm) × t” (2.5 mm nominal) is obtained from the VARTM CFVE panel in a target orientation. It can be cut in the direction of warp to get the 0^0 sample, perpendicular to the direction of warp to get the 90^0 sample or at an angle of 45^0 to the warp.

Specimens from two different panels were evaluated as shown in Table 5. Part of the specimens were time aged (dry) while other specimens from a given panel and location and orientation were soaked in sea water at 40 °C for several weeks (wet) till the moisture uptake reached saturation equilibrium monitored by periodic weight gain data. Many tests were conducted prior to obtaining the compression response summarized in Table 5 during the process of perfecting the process to conduct highly reliable compression testing using CLC fixture. Testing improvements included procedures to fabricate and assemble flat specimens in test fixture with minimum misalignment, torque controlled gripping for repeatable lateral restraint in the grip

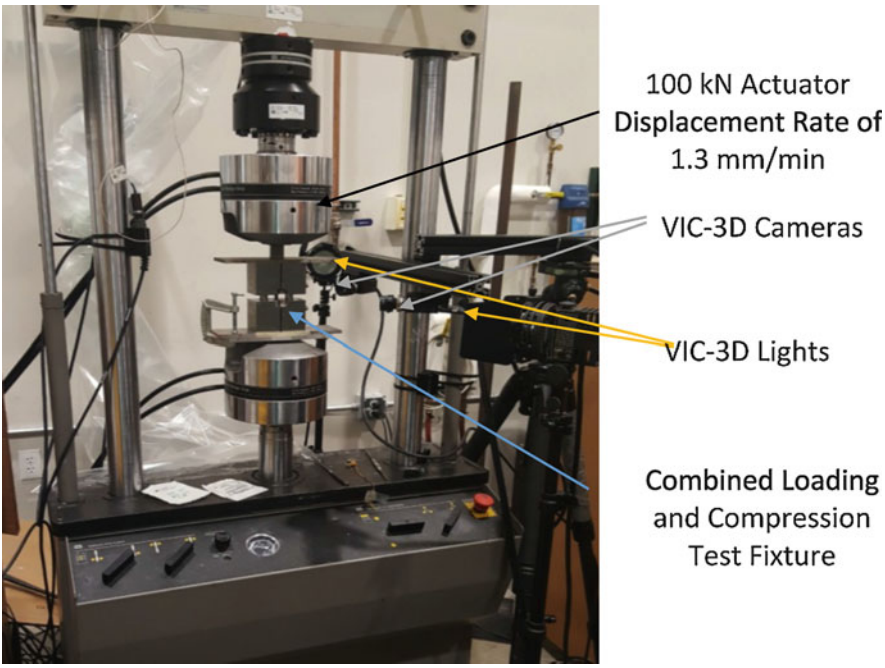

Fig. 27 Compression testing setup with spatially resolved strain mapping

Table 5 Summary results of compression behavior and sea water effects

Panel	Environment	Specimen Orientation (degrees)	Compression Modulus (GPa) Average Value	Compression Strength (MPa) Average Value	Compression Strength Degradation Due to Sea Water (%)
			Compression Modulus from Individual Tests	Failure Stress from Individual Tests	
Panel 1	Dry	0	49.35	399	
			41 | 57.7	461 | 237	
Panel 2	Dry	0	49	461	
			52.2 | 56.6 | 44.5 | 44.2 | 48	464.3 | 455.9 | 492.52 | 389 | 502.88	
Panel 1	Wet	0	43.75	269	32
			44.6 | 42.9	278 | 260	
Panel 2	Wet	0	57.4	349	24.3
			57.4	349	
Panel 1	Dry	45	11.6	127	
			10.3 | 13.4 | 10.6 | 10.6	129 | 125 | 160 | 125	
Panel 2	Dry	45	14.96	124	
			15.2 | 18.3 | 11.2 | 14.2 | 15.7	120.68 | 122.7 | 126.9 | 123 | 127.4	
Panel 1	Wet	45	11.55	118.5	7
			11 | 12.1	121 | 116	
Panel 2	Wet	45	14.55	118.1	4.7
			15.1 | 14	114.9 | 121.3	
Panel 1	Dry	90	46.96	422	
			46.1 | 48.6 | 52.2 | 46.6 | 41.3	431 | 450 | 462 | 376 | 389	
Panel 2	Dry	90	55.5	489	
			54.2 | 55.5 | 58.7 | 53.5	552.35 | 487.7 | 453.9 | 462.5	
Panel 1	Wet	90	47.35	415	1.6
			48.1 | 46.6	435 | 395	
Panel 2	Wet	90	56.1	444	9.2
			54.9 | 57.3	488.6 | 399.2	

regions, procedures to mount strain gage rosettes on the gage section, and simultaneously obtaining spatially resolved strains during CLC testing, first of its kind in this study. As can be seen from Table 1, there was consistent difference in

compression properties for Panels 1 and 2 though they were identically prepared during the manufacturing using vary carefully controlled VARTM process. For a given panel, specimens that were exposed to long-term sea water showed substantial degradation in compressive strength for fiber dominated samples $[0/90]_{2S}$, with a loss in compressive strength in the range of 24% and 32% for Panel 1, and 1.5% & 9.2% for Panel 2. Currently detailed evaluation of the role of microstructure and corresponding failure modes is ongoing to ascertain such large difference for observed average degradation in strength for two panels. For matrix dominated samples $[\pm 45]_{2S}$, the degradation in compressive strength was found to be 4.7% and 7% and is much less pronounced. The tensile response of these composites under identical manufacturing conditions show much less degradation in fiber direction and similar degradation in the matrix direction. The ingress of water is associated with increased separation between the molecular chains, thereby inducing expansion strains and may have significantly more deleterious effect in compression. This is a very important finding and the root cause of the measured degradation will require further evaluation of the effect on matrix and fiber-matrix interface as well. An example result of axial strain measured during two load-unload cycles during a compression test for one of the $[0/90]_{2S}$ specimens is shown in Fig. 28.

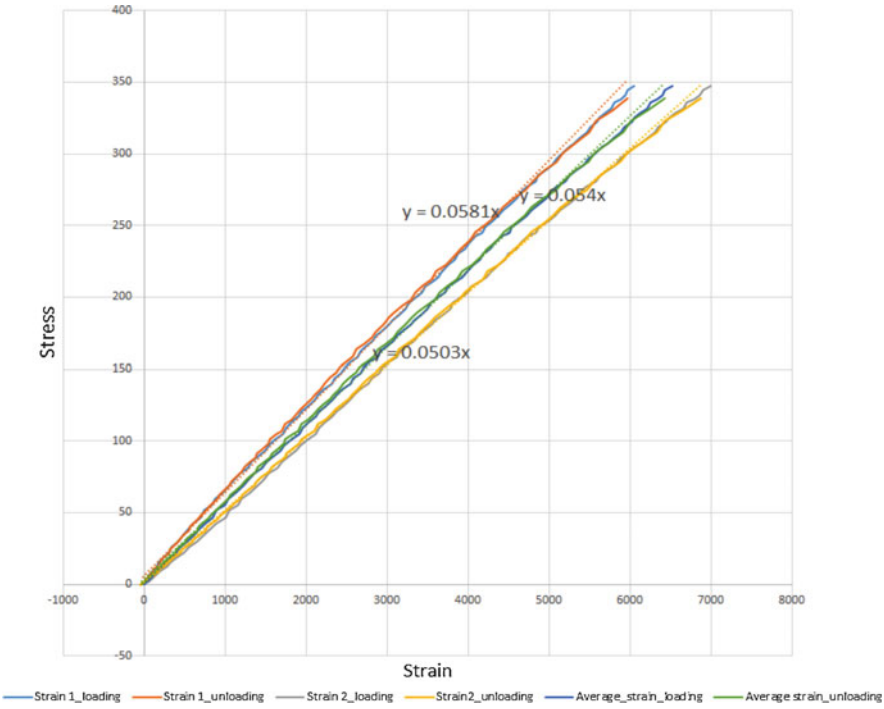

Fig. 28 Compressive stress-strain data from two strain gages mounted front and back sides of the specimen, and average compressive strain showing the effects of small misalignments during a CLC based compression test

Since the tensile strength of approximately 1 GPa was reduced by 60% for fiber dominated $[0/90]_{2S}$, it appears that the resulting microstructure at fiber tow level using VARTM approach with relatively large aerial density biaxial fabric is impacting the loss in strength in compression loading substantially. Currently detailed investigation of interpreting the initial compression data reported above considering strain gage data, spatially resolved 3D-DIC, and microstructure evaluations using high resolution computed X-ray tomography is ongoing. It is expected that the results will lead to important basic understanding of characterizing compression behavior of composites and degradation from harsh marine environment.

9 Summary

Mechanical degradation of polymeric composites was experimentally investigated due to exposure to sea environment and low temperature over extended period of time. Following observations are summarized associated with static, fracture, fatigue loading in tension, and degradation in compression response from seawater exposure.

- Only the outer boundary of PVC foam core was penetrated and degraded by the sea water for long-term exposure (several years) while the inner part still remained dry. The shear and Young's moduli of polymeric foam were tested by means of novel techniques and found to be $G = 25$ MPa and $E = 60$ MPa, respectively. Exposure to sea environment and low temperature resulted in approximate 8% degradation under torsion but no significant reduction could be detected under tensile tests. σ_{failure} of foam core was approximately 2.5 MPa and reduced up to 10% due to sea environment. No significant reduction is found when combined effects of sea and low temperature environment.
- Elastic properties of carbon fiber and resin dominated samples, $[0/90]_{2s}$ and $[\pm 45]_{2s}$, were insensitive to coupling effects. However, it was shown that σ_{failure} of $[\pm 45]_{2s}$ decreased by 5% due to sea water and has slightly reduced further with subsequent freezing after soaking.
- It has been shown that the interfacial fracture toughness G_c of sandwich structure decreased by 30% due to sea environment. The result indicated that exposure to sea water may severely reduce the interfacial toughness.
- Fatigue life of CF/VE composite samples on $[\pm 45]_{2S}$, which have the average static failure strength at 120 MPa, were obtained at maximum applied stress levels of 0.8, 0.67, 0.6, and 0.5 under tension-tension cyclic loading. Fatigue life due to sea water confinement and one-sided confined effects is evaluated against response from cyclic loading in air. A significant degradation of number of cycles to failure from sea water confinement effects was observed for all stress levels considered in this study up to 80% of static strength as the maximum cyclic stress value for a stress ratio of 0.1.

- A combined load compression fixture integrated with most advanced imaging and radiation based measurements systems is established for the study of marine composites under compression.
- The degradation associated with long-term exposure to sea water on the compression behavior of composite facings and tensile fatigue behavior of sandwich structures under one sided exposure was evaluated using very carefully controlled experimental data and advanced mechanics based modeling. The effect of sea water on CF/VE facings was evaluated for elastic and failure behavior in compression at different orientation of layups using an integrated approach of obtaining deformation data using on specimen strain gages on front and back face of the CLC specimens, spatially resolved 3-D digital image correlation, and microstructural changes and associated failure modes using high resolution and non-invasive computed tomography techniques.
- Substantial degradation of compression strength in both fiber and matrix dominated orientations for the carbon fiber reinforced vinyl ester composite laminates has been observed and microstructural investigations are currently underway to ascertain the dominant failure modes associated with each sample failed in compression. Noticeable variation in compression properties were observed for two different panels made using identical VARTM protocols, but for a given panel, there was a consistent and substantial degradation in compression strength due to long term sea water soaking.
- Monotonic tensile loading on composite facings on sandwich structures using a custom developed specimen configuration from a sandwich structure shows monotonic tensile modulus and failure strength considerably smaller than the conditions associated with identical laminate only manufacturing technique. Detailed microstructure from x-ray computed tomography verified the cause for the loss in tensile properties associated with sandwich facings and this aspect needs to be considered carefully for naval design.
- One sided water exposure and corresponding degradation in tensile fatigue life for these facings was also obtained for a constant R ratio and a maximum cyclic stress of 67% of the tensile strength.

Acknowledgments This research was supported by ONR Contracts through Solid Mechanics Program for the past decade, under a program managed by Dr. Yapa Rajapakse and is gratefully acknowledged. Majority of the material presented in this chapter was based on doctoral student's research work of Dr. Akawat Siriruk, Mr. Vivek Chawla, and Mr. Zachary Arwood and is greatly appreciated. Dr. Penumadu also would like to acknowledge the indirect support to this research from US Department of Energy and National Science Foundation for related investments in his fiber reinforced composites research program, resources, and facilities and more recently from the Institute for Advanced Composites Manufacturing Innovation.

References

1. Li X, Weitsman YJ (2004) Sea-water effects on foam-cored composite sandwich lay-ups. Compos Part B 35(6–8):451–459
2. Weitsman YJ (2012) Effects of fluids on mechanical properties and performance fluid effects in polymers and polymeric composites. Springer, Boston
3. DIAB Divinycell, Divinycell International, DeSoto, TX, USA
4. Shivakumar KN, Swaminathan G, Sharpe M (2006) Carbon/vinyl ester composites for enhanced performance in marine applications. J Reinf Plast Compos 25(10):1101–1116
5. Wood CA, Bradley WL (1997) Determination of the effect of seawater on the interfacial strength of an interlayer E-glass/graphite/epoxy composite by in situ observation of transverse cracking in an environmental SEM. Compos Sci Technol 57(8):1033–1043
6. Siriruk A, Penumadu D, Jack Weitsman Y (2009) Effect of sea environment on interfacial delamination behavior of polymeric sandwich structures. Compos Sci Technol 69(6):821–828
7. Siriruk A, Weitsman YJ, Penumadu D (2009) Polymeric foams and sandwich composites: material properties, environmental effects, and shear-lag modeling. Compos Sci Technol 69 (6):814–820
8. Guedes RM (2007) Durability of polymer matrix composites: viscoelastic effect on static and fatigue loading. Compos Sci Technol 67(11–12):2574–2583
9. Hwang W, Han KS (1986) Fatigue of composites—fatigue Modulus concept and life prediction. J Compos Mater 20(2):154–165
10. Lee LJ, Yang JN, Sheu DY (1993) Prediction of fatigue life for matrix-dominated composite laminates. Compos Sci Technol 46(1):21–28
11. Petermann J, Schulte K (2002) The effects of creep and fatigue stress ratio on the long-term behaviour of angle-ply CFRP. Compos Struct 57(1–4):205–210
12. Siriruk A, Penumadu D (2014) Degradation in fatigue behavior of carbon fiber–vinyl ester based composites due to sea environment. Compos Part B 61(0):94–98
13. Lee LJ, Fu KE, Yang JN (1996) Prediction of fatigue damage and life for composite laminates under service loading spectra. Compos Sci Technol 56(6):635–648